ELSEVIER

Journal of Biomechanics 37 (2004) 495–501

JOURNAL OF BIOMECHANICS

www.elsevier.com/locate/jbiomech
www.JBiomech.com

Numerical investigation of the intravascular coronary stent flexibility

Lorenza Petrini[a,*], Francesco Migliavacca[b], Ferdinando Auricchio[a], Gabriele Dubini[b]

[a] *Dipartimento di Meccanica Strutturale, Università degli Studi di Pavia, Via Ferrata 1, Pavia 27100, Italy*
[b] *Dipartimento di Bioingegneria e Ingegneria Strutturale, Laboratory of Biological Structure Mechanics, Politecnico di Milano, Milan, Italy*

Accepted 1 September 2003

Abstract

Nowadays stent therapy is widely adopted to treat atherosclerotic vessel diseases. The high commercial value of these devices and the high prototypation costs require the use of finite element analyses, instead of classical trial and error technique, to design and verify new models. In this paper, we explore the advantages of the finite element method (FEM) in order to investigate new generation stent performance in terms of flexibility. Indeed, the ability of the stent to bend in order to accommodate curvatures and angles of vessels during delivery is one of the most significant prerequisites for optimal stent performance. Two different FEM models, resembling two new generation intravascular stents, were developed. The main model dimensions were obtained by means of a stereo microscope, analyzing one Cordis BX-Velocity and one Carbostent Sirius coronary stent. Bending tests under displacement control in the unexpanded and expanded configuration were carried out. The curvature index, defined as the ratio between the sum of rotation angles at the extremes and the length of the stent, yielded comparative information about the capability of the device to be delivered into tortuous vessels and to conform to their contours. Results, expressed in terms of the bending moment-curvature index, demonstrated a different response for the two models. In particular the Cordis model showed a higher flexibility. Lower flexibility in the expanded configurations for both models was detected. However this flexibility depends on how the contact takes place between the different parts of the struts.

Keywords: Stent flexibility; Coronary stent; Finite element method; Mechanical response; Mathematical model

1. Introduction

Stents are tubes made out of wire or by cutting laser meshes that are inserted into arteries to help keep them open so blood can flow properly. An angioplasty procedure to open up a clogged artery is often performed before the stent is inserted, with the stent providing a tiny frame, acting like support beams in a mine, to help keep the walls of the re-opened artery in place. Although stents are now commonly used, they are not a panacea. Sometimes arteries will still become clogged and narrowed again even with a stent (Gershlick, 2002). This phenomenon is called "restenosis." Recently, restenosis has been reduced with the introduction of stents coated with specific drugs (Regar et al., 2001; Bailey, 2002).

Optimization of stent mechanical properties can surely lead to a better long-term efficacy of the device itself. In this context, computational fluid dynamics (Natarajan and Mokhtarzadeh-Dehghan, 2000; Frank et al., 2002) and structural analyses (Dumoulin and Cochelin, 2000; Auricchio et al., 2001; Tan et al., 2001; Migliavacca et al., 2002; Prendergast et al., 2003), based, for example, on the finite element method (FEM), are useful tools to reach this target. Indeed, computational analyses could provide access to an extensive amount of information under highly controlled conditions, thus, making it possible to screen different and competing coronary stent design alternatives prior to costly prototype fabrication. On the other hand, due to the lack of sophisticated and often *ad hoc* numerical methods capable of handling the complexity of real-life stent behavior, up to now designers have only used computational analyses after prototype fabrication to provide further understanding of typical stent performance (Bartorelli et al., 2000). Therefore, a critical

*Corresponding author. Tel.: +39-382-505475; fax: +39-382-528422.
E-mail address: petrini@unipv.it (L. Petrini).

0021-9290/$ - see front matter © 2003 Published by Elsevier Ltd.
doi:10.1016/j.jbiomech.2003.09.002

requirement for a numerical code, which is necessary to reach its full potential with regards to the stent simulation, is the development of accurate and efficient algorithms capable of simulating the real stent expansion, recoil, flexibility, interaction with human vessels, etc. Accordingly, this paper investigates the potentials of the FEM to determine stent flexibility. Indeed, flexibility is one of the prerequisites for coronary stents: it is the ability to bend in order to accommodate a turn or angle which is required to deliver the stent and to conform with the vessel after the stent is deployed. These properties are related to the trackability of the stent, which refers to the ability of the system to advance distally around a guidewire, while following the guidewire tip along the path of the vessel, which can include narrow, tortuous passages. In scientific literature some experimental methods were proposed with the aim of evaluating mechanical properties of the intravascular stents, among which flexibility was also investigated (Flueckiger et al., 1994; Ormiston et al., 1998; Ormiston et al., 2000; Dyet et al., 2000; Duda et al., 2000). Those studies were based on quantitative comparison of different designs. With regards to numerical studies, literature is very scarce. The only study regarding the flexibility of coronary stents was proposed by Etave et al. (2001) in idealized tubular and coil stents.

In our paper FEM is exploited to investigate and compare the flexibility of two new generation balloon-expandable coronary stents, both in the expanded and unexpanded configuration. This approach can be easily applied to most coronary stent designs.

2. Materials and methods

Two three-dimensional models resembling two new generation intravascular stents (Cordis BX-Velocity, Johnson & Johnson, Interventional System, Warren, NJ, USA and Sirius Carbostent, Sorin Biomedica, Saluggia, VC, Italy) are considered. The two 3D models will be denoted as CV and SC, respectively. The term 'new generation' defines all stents with a structure in which it is possible to recognize the presence of two different types of elements: (i) tubular-like rings and (ii) bridging members (links). The former mainly functions to sustain the vessel after the stent expansion and the latter to link the rings in a flexible way during the delivery process. Hence, each one, respectively, determine the stiffness and the flexibility of the overall structure.

In particular, when a stent passes through or it is expanded in a curved vessel, the links adjust to follow the curved path while the rings mainly remain straight; if the vessel is sufficiently curved to induce stresses beyond the yield limit of the material, the links are plastically deformed and the structure tends to behave as a series of rigid bodies (the rings) connected by hinges (the links). On the basis of these considerations it is reasonable and computationally convenient to study the flexibility by observing only a portion of the stent model, which we will refer to as a unit, composed of two rings and the links between them. However, this hypothesis will be verified in the conclusion of this study.

The units of the two intravascular stents herein studied are depicted in Fig. 1 in their unexpanded and expanded configurations. To obtain the main dimen-

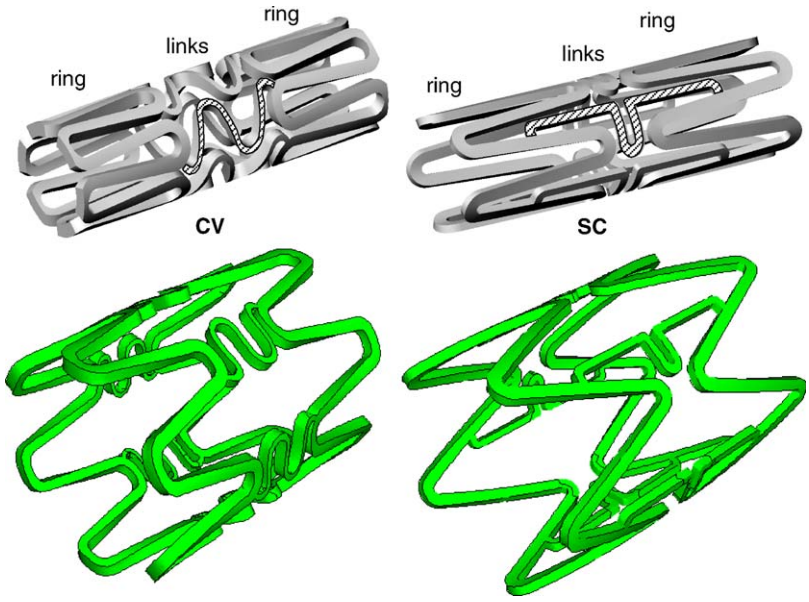

Fig. 1. Geometries of the CV and SC models in the unexpanded (top) and expanded (bottom) configurations. The dashed areas enlighten a link of the stent.

sions of the models, one Cordis BX-Velocity and one Carbostent Sirius coronary stent were analyzed through the use of a Nikon SMZ800 stereo microscope (Nikon Corporation, Tokyo, Japan). The geometry of the two models were created using Rhinoceros 1.1 Evaluation CAD program (McNeel & Associates, Indianapolis, IN, USA) on the basis of the microscopic analysis. The CV model is characterized by rings connected at the top by six links (Fig. 1). The inner diameter in the unexpanded configuration is 0.9 mm while the thickness of the stents is 0.14 mm. The expanded configuration has an outer diameter equal to 2.5 mm. The SC model contains rings connected in the middle by five links (Fig. 1). The inner diameter in the unexpanded configuration is 1.0 mm while the thickness of the stents is 0.1 mm. The expanded configuration has an outer diameter equal to 2.5 mm.

The stents are made of 3161 stainless steel. The inelastic constitutive response is described through a Von Mises–Hill plasticity model with isotropic hardening. The Young modulus is 196 GPa, the Poisson ratio is 0.3, the yield stress is 205 MPa (Auricchio et al., 2001).

The models were meshed with 10-node tetrahedral elements. Depending on the geometry of the model, the number of nodes was in the range between 31,871 and 77,228, while elements were between 14,704 and 39,398. Element skewness was always smaller than 0.90. The meshes were automatically generated by GAMBIT commercial code (Fluent Inc., Lebanon, NH, USA). The number of nodes and elements is sufficiently high to have a solution independent from the mesh grid as already shown in a previous study of ours (Migliavacca et al., 2002). In that work different stent models were analyzed with a length five times longer than the CV and SC models used here and were discretized with a number of elements no greater than 40,000 in the most complicated model.

A large deformation analysis is performed using ABAQUS commercial code (Hibbit Karlsson & Sorenses, Inc., Pawtucket, RI, USA) based on the FEM. In particular, the ABAQUS/Standard program is used in the classical displacement formulation. The nonlinear problem, due to material plasticity and contact constraint, is solved using a Newton–Raphson's method. The method convergence criterion consists of ensuring that the largest residual in the balance equations and the largest correction to any nodal unknown provided by the current Newton iteration are sufficiently small. In particular, for the studied problem the convergence is verified when the residual force is less than a predefined tolerance (in our case 0.5% of the average force in the structure, averaged over space and time) and when the largest displacement correction is less than a predefined tolerance (in our case 10% of the largest incremental displacement). To model possible interactions between specific model portions, specific frictionless contact surfaces are introduced. The contact constraint is defined by using the Lagrange multiplier approach, so that the constraint variable is the normal pressure and the constraint is the surface penetration. In particular, the ABAQUS finite-sliding contact option, which allows for the separation and sliding of finite amplitude, along with arbitrary rotation, between two 3D deformable body surfaces, was adopted.

The goal of the simulation is to provide a measurement of the stent flexibility: with the aim to simulate the constraint of the curved vessel on the stent, a bending deformation was imposed on the stent model and the corresponding bending loading was computed. Accordingly, the analyses were performed under displacement control: the extremes of the models sketched in Fig. 2 were rotated at a fixed angle φ. The choice of the rotation axes was dependent on the geometry of the stent and, in particular, on the position of the links. Indeed, the main effect, during the increase of the rotation angle φ, is the elongation of the link (or links) in the positive flexural plane and the contraction of the opposite link (or links) until link self-contact or contact between nearby links takes place. This contact may also be between links and rings. While considering how contact takes place, we selected the following two cases at the limit in terms of differences in the model responses under bending tests (Fig. 3):

- a rotation around the x-axis;
- a rotation around the y-axis.

Two sets of simulations were performed:

- a bending test in the unexpanded configuration;
- a bending test in the expanded configuration.

Simulations were carried out with an increase of rotation up to 20° in the case of unexpanded stents and 10° in the case of expanded stents. The expanded configurations were obtained imposing a displacement to the external nodes on the unexpanded models up to an outer stent diameter equal to 2.5 mm. Results were expressed in terms of bending moment (M) at the extremes as a function of the curvature index:

$$\chi = \Delta\varphi / L,$$

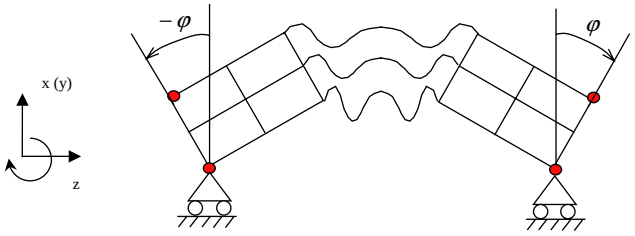

Fig. 2. Sketches of the stent unit with angle of rotation φ.

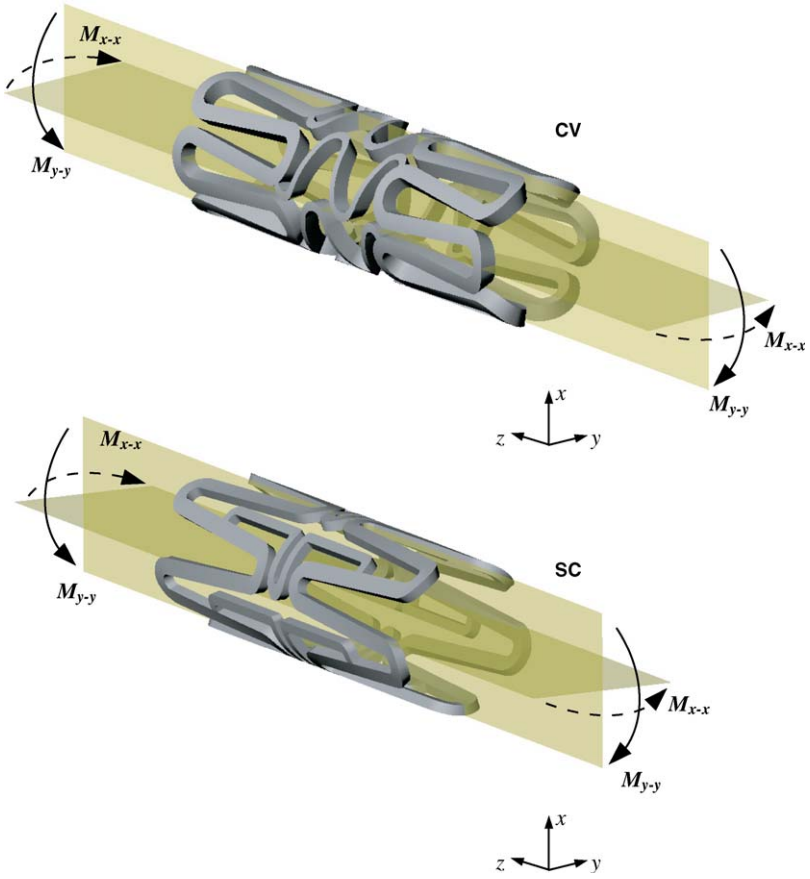

Fig. 3. Planes of application of bending for the CV (top) and SC (bottom) models.

where $\Delta\varphi$ is equal to 2φ and L is the length of the unit. The slope of the curve $M-\chi$ measures the stent stiffness, that is the reciprocal of flexibility. In particular, two slopes were obtained from the best straight line that could fit on the drawn the curve $M-\chi$. The first slope is related to the stiffness of the stent in the elastic range, while the second is related to the stiffness of the stent in the plastic range.

3. Results and discussion

3.1. Flexibility in the unexpanded configuration

Fig. 4 shows the curves $M-\chi$ for the CV and the SC models for a bending around the x and y axes; the numerical results in terms of flexibility are reported in Table 1. Fig. 5 depicts the geometries of the deformed stent with the Von Mises stresses reached at a curvature index $\chi = 0.06\,\mathrm{rad\,mm^{-1}}$ for bending around the x-axis; the figure insets show contact details of the models.

From the obtained results it is possible to conclude that the CV model demonstrates a response independent from the axis of rotation. On the contrary, the SC model exhibits a different response according to the selected

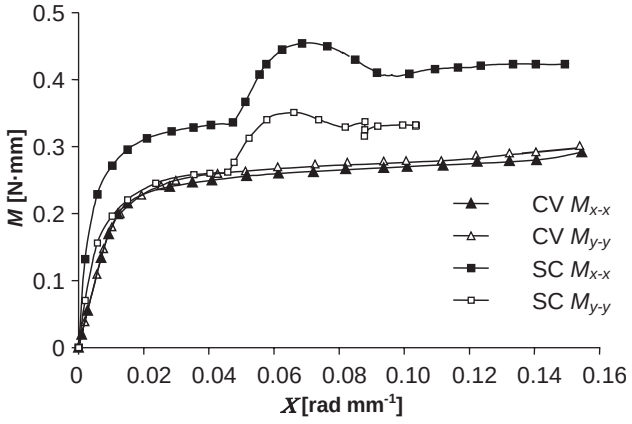

Fig. 4. Moment–curvature index curves relative to the CV and SC models in the unexpanded configuration.

rotation axis. This can be explained considering the different stent geometries (Fig. 1) and their variations during the bending. Indeed, the links of the CV have two crests and are connected with the top of the ring, while the links of the SC model have only one crest and are connected with the center of the ring. As a consequence, the CV links exhibit a high capability to deform independently from the rings: during bending, stresses

Table 1
Flexibility values of unexpanded models derived from the moment–curvature index curves of Fig. 4

Model	Rotation axis	Elastic field flexibility (rad N^{-1} mm^{-2})	Plastic field flexibility (rad N^{-1} mm^{-2})
CV	x	0.052	3.87
CV	y	0.052	4.45
SC	x	0.015	0.75
SC	y	0.029	2.74

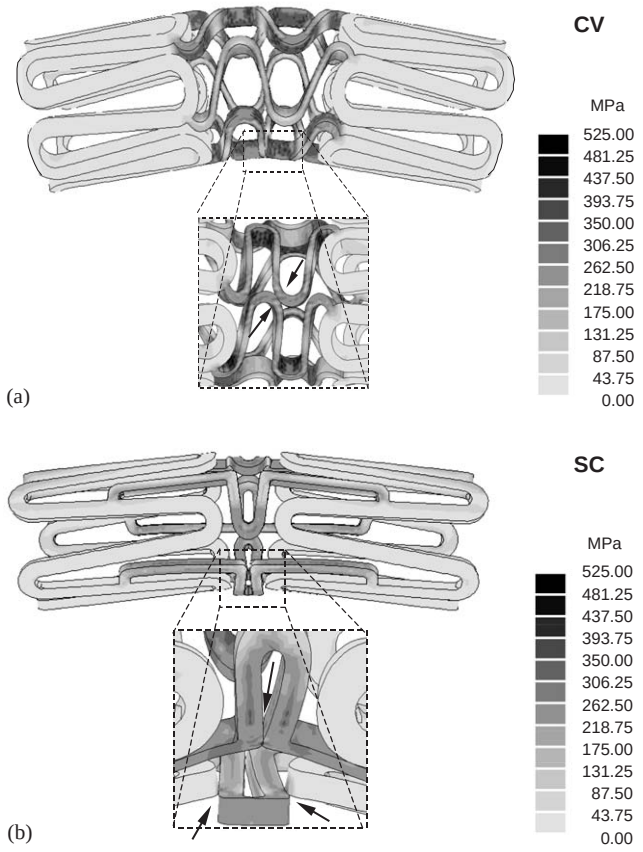

Fig. 5. Von Mises stresses at a curvature index $\chi = 0.06\,\mathrm{rad\,mm^{-1}}$ for the CV (a) and SC (b) models in the unexpanded configuration during bending around the x-axis. Arrows in the reverse view enlargements indicate the areas of contact.

(and strains) are concentrated in the links and increase in a continuous way as the material plastically deforms, while the rings remain unstressed (and unstrained) (Fig. 5a). The contact takes place only between the links and at high rotation values (about 12°, $\chi = 0.14\,\mathrm{rad\,mm^{-1}}$). This explains the independence of the test results from the rotation axis and the smoothness of the $M-\chi$ curve (Fig. 4). In the SC model, on the contrary, rings and links do not deform independently: during bending, stresses (and strains) develop both in the links and in the segments of the rings connected to the links (Fig. 5b). As it was expected, the stiffness of the structure is higher for rotation around the x-axis, when the straight segments of the rings are in the zone of maximum and minimum stress (bending plane $y-z$) (Fig. 3b). In both rotation cases a self-contact of a single link takes place at small rotations (about 8°, $\chi = 0.05\,\mathrm{rad\,mm^{-1}}$), which causes a discontinuity in the $M-\chi$ curves and a strong increment in the slopes (Fig. 4). The flexibility in the plastic range is calculated before self-contact occurs. Increasing φ, the curves show a softening behavior. This is connected to an instability phenomenon due to the rings which, during their rotation, push the previously mentioned single link inwards.

3.2. Flexibility in the expanded configuration

The $M-\chi$ curves from the performed tests are depicted in Fig. 6 with the numerical flexibility results reported in Table 2. Fig. 7 depicts the geometries of the deformed stent with the Von Mises stresses reached at a curvature index $\chi = 0.03\,\mathrm{rad\,mm^{-1}}$ for bending around the x-axis with the figure insets depicting contact details of the models.

The expanded configuration responses demonstrate a tendency similar to the unexpanded ones, but with a lower flexibility. Accordingly, the CV model depicts stresses which are concentrated in the links, with bending moment increasing in a continuous way; the contact takes place at high rotation values, between

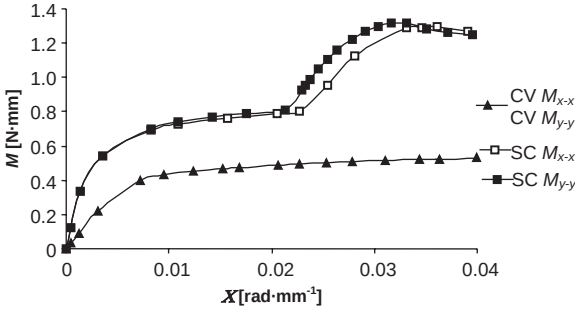

Fig. 6. Moment–curvature index curves relative to the CV and SC models in the expanded configuration.

Table 2
Flexibility values of expanded models derived from the moment-curvature index curves of Fig. 6

Model	Rotation axis	Elastic field flexibility (rad N^{-1} mm^{-2})	Plastic field flexibility (rad N^{-1} mm^{-2})
CV	x	0.0138	0.383
CV	y	0.0138	0.383
SC	x	0.0042	0.161
SC	y	0.0041	0.154

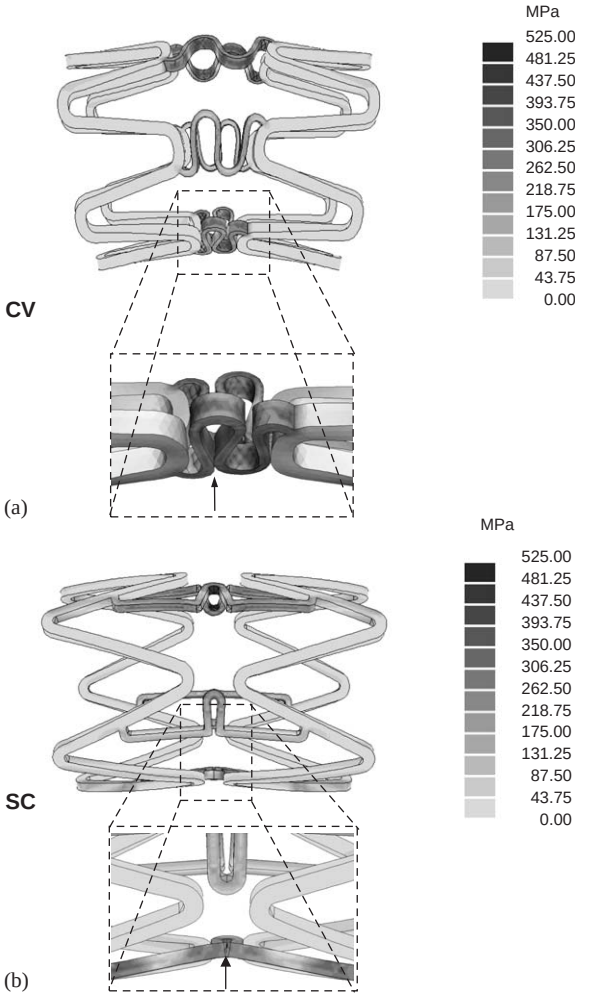

Fig. 7. Von Mises stresses at a curvature index $\chi = 0.03\,\mathrm{rad\,mm^{-1}}$ for the CV (a) and SC (b) models in the expanded configuration during bending around the x-axis. Arrows in the reverse view enlargements indicate the areas of contact.

parts of the same link (arrow in Fig. 7a). In the SC model, two links have self-contact at low rotation (Fig. 7b) and, again, this causes a sudden increase in stiffness, followed by instability phenomena (Fig. 6).

4. Conclusions

The proposed approach allows to evaluate the index of flexibility of different new generation stents both when the material is elastically deformed (smaller rotation) or plastically deformed (larger rotation). The unique structure of the new generation stents allows one to study flexibility of the stent while examining only a unit of the model, which leads to a large reduction of the computational costs. To confirm this approach, a bending test around y-axis on a complete CV model (5 links and 6 rings) in the unexpanded configuration was performed. In Fig. 8 the $M-\chi$ curves of the whole stent

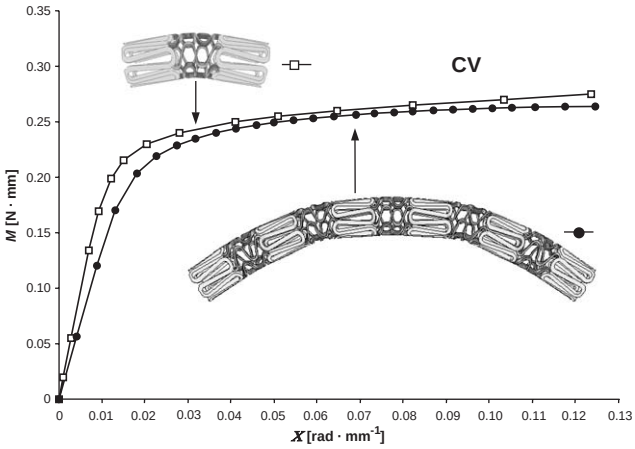

Fig. 8. Moment–curvature index curves for a single unit (squares) and a complete structure (6 rings and 5 links, circle) of the CV model.

and of the single unit are compared. The capability of the single unit to reproduce a behavior similar to that of the overall stent underlines the usefulness of a simpler model in determining the flexibility of stents, especially for comparative analyses.

The performed tests on the two models suggest that the methodology is able to resolve quantitatively the local details in stent structural behavior, even if a validation should include a comparison between experimental and computational tests carried out on the same stents. It is important to underline here the necessity to know exactly the geometry of the stent so as to perform a correct analysis; indeed, design influences flexibility as shown in this study. In this regard the two investigated models have different thicknesses, which have implications in the stent response during bending.

The main limitation of this work is the absence of the delivery system during the flexibility analysis in the unexpanded configuration. Indeed, testing of manufacturer-mounted stents showed (Dyet et al., 2000) that the presence of a catheter influences the structure during the stent advancing phase.

As a conclusive remark, it is possible to confirm the dependency of the flexibility on the position and shape of the links as well as on the way in which contact between the parts of the structure takes place.

Acknowledgements

The authors would like to thank Valeria Montanari, MEng, Isabella Quagliana, MEng, Paolo Massarotti MEng and Silvia Schievano MEng for their contribution to model development and numerical analyses.

References

Auricchio, F., Di Loreto, M., Sacco, E., 2001. Finite-element analysis of a stenotic artery revascularization through a stent insertion. Computer Methods in Biomechanics and Biomedical Engineering 4, 249–263.

Bailey, S.R., 2002. Coronary restenosis: a review of current insights and therapies. Catheterization and Cardiovascular Interventions 55, 265–271.

Bartorelli, A.L., Virmani, R., Antoniucci, D., 2000. The sorin carbostent. In: Serruys, P.W., Kutryk, M.J.B. (Eds.), Handbook of Coronary Stents, 3rd Edition. Martin Dunitz Ltd., London, pp. 177–186.

Duda, S.H., Wiskirchen, J., Tepe, G., Bitzer, M., Kaulich, T.W., Stoeckel, D., Claussen, C.D., 2000. Physical properties of endovascular stents: an experimental comparison. Journal of Vascular and Interventional Radiology 115, 645–654.

Dumoulin, C., Cochelin, B., 2000. Mechanical behaviour modelling of balloon-expandable stents. Journal of Biomechanics 33, 1461–1470.

Dyet, J.F., Watts, W.G., Ettles, D.F., Nicholson, A.A., 2000. Mechanical properties of metallic stents: how do these properties influence the choice of stent for specific lesions? Cardiovascular and Interventional Radiology 23, 47–54.

Etave, F., Finet, G., Boivin, M., Boyer, J.C., Rioufol, G., Thollet, G., 2001. Mechanical properties of coronary stents determined by using finite element analysis. Journal of Biomechanics 34, 1065–1075.

Flueckiger, F., Sternthal, H., Klein, G.E., Aschauer, M., Szolar, D., Kleinhappl, G., 1994. Strength, elasticity, and plasticity of expandable metal stents: in vitro studies with three types of stress. Journal of Vascular and Interventional Radiology 5, 745–750.

Frank, A.O., Walsh, P.W., Moore, J.E., 2002. Computational fluid dynamics and stent design. Artificial Organs 26, 614–621.

Gershlick, A.H., 2002. Treating atherosclerosis: local drug delivery from laboratory studies to clinical trials. Atherosclerosis 160, 259–271.

Migliavacca, F., Petrini, L., Colombo, M., Auricchio, F., Pietrabissa, R., 2002. Mechanical behavior of coronary stents investigated through the finite element method. Journal of Biomechanics 35, 803–811.

Natarajan, S., Mokhtarzadeh-Dehghan, M.R., 2000. A numerical and experimental study of periodic flow in a model of a corrugated vessel with application to stented arteries. Medical Engineering & Physics 22, 555–566.

Ormiston, J.A., Ruygrok, P.N., Webster, M.W., Stewart, J.T., White, H.D., 1998. Mechanical properties of five long stents compared. Journal of Invasive Cardiology 10 (Suppl. B), 35B.

Ormiston J, A., Dixon, S.R., Webster, M.W., Ruygrok, P.N., Stewart, J.T., Minchington, I., West, T., 2000. Stent longitudinal flexibility: a comparison of 13 stent designs before and after balloon expansion. Catheterization and Cardiovascular Interventions 50, 120–124.

Prendergast, P.J., Lally, C., Daly, S., Reid, A.J., Lee, T.C., Quinn, D., Dolan, F., 2003. Analysis of prolapse in cardiovascular stents: a constitutive equation for vascular tissue and finite-element modeling. Journal of Biomechanical Engineering 125, 692–699.

Regar, E., Sianos, G., Serruys, P.W., 2001. Stent development and local drug delivery. British Medical Bulletin 59, 227–35248.

Tan, L.B., Webb, D.C., Kormi, K., Al-Hassani, S.T., 2001. A method for investigating the mechanical properties of intracoronary stents using finite element numerical simulation. International Journal of Cardiology 78, 51–67.